Plant Systematics and Evolution
https://doi.org/10.1007/s00606-018-1545-9

ORIGINAL ARTICLE

Differentiation of the endemic Greek genus *Hymenonema* and its relatives of subtribe Scolyminae (Compositae, Cichorieae) based on a multilocus species tree reconstruction

Eleni Liveri[1] · Salvatore Tomasello[2,3] · Christian Hammerschmid[2] · Georgia Kamari[1] · Christoph Oberprieler[2]

Received: 15 February 2018 / Accepted: 17 September 2018

Abstract

Hymenonema (Compositae, tribe Cichorieae) together with the genera *Catananche*, *Gundelia*, and *Scolymus* forms the subtribe Scolyminae. It is endemic to Greece and consists of two species, *Hymenonema laconicum* and *Hymenonema graecum*, which occur in the south Peloponnisos and central Aegean area, respectively. The present contribution aims at a phylogenetic reconstruction of evolutionary relationships among the 12 species of the subtribe, focusing on the temporal and spatial framework for its evolution. The phylogenetic relationships among the members of Scolyminae were inferred from molecular data based on the multi-copy region of the nrDNA internal transcribed spacers ITS1 and ITS2, two intergenic spacers of the cpDNA (*trn*L-*trn*F, *rpl*32-*trn*L), and one single-copy nuclear region (*D10*). The gene trees were reconstructed using Bayesian phylogenetic methods. All gene trees support the monophyly of *Hymenonema* and the sister-group relationship with the genus *Scolymus*. The further sister-group relationship of this group (*Hymenonema–Scolymus*) with *Catananche* is also supported by nrDNA and cpDNA analyses. Finally, a species tree (inferred in a Bayesian coalescent framework) was reconstructed and dates the divergence time between the two *Hymenonema* species to the Pleistocene (around 1.3 Ma ago). Maximum likelihood-based biogeographical reconstructions suggest a Miocene (pre-Messinian) differentiation of the subtribe on the northern Tethyan platform, followed by Miocene/Pliocene dispersal events to the western Mediterranean and North-African platforms and final, small-scale vicariance events within the genera in the Pleistocene.

Keywords Aegean · Asteraceae · Biogeography · Phylogeny · Pleistocene · Pliocene

Introduction

Narrow endemism is the cornerstone of plant diversity in the Mediterranean area, and its geographical patterns and their geological, climatological, and ecological correlates are fundamental for understanding the region's plant biogeography, evolutionary biology, and conservation biology (Thompson 2005). In this respect, small, and in many cases unispecific

Handling Editor: Terry A.J. Hedderson.

Electronic supplementary material The online version of this article (https://doi.org/10.1007/s00606-018-1545-9) contains supplementary material, which is available to authorized users.

✉ Christoph Oberprieler
christoph.oberprieler@ur.de

Eleni Liveri
eleniliveri@upatras.gr

Salvatore Tomasello
salvatore.tomasello@uni-goettingen.de

Christian Hammerschmid
christian.hammerschmid@rwth-aachen.de

Georgia Kamari
kamari@upatras.gr

[1] Department of Biology, Section of Plant Biology, University of Patras, 26504 Rio, Greece

[2] Evolutionary and Systematic Botany Group, Institute of Plant Sciences, University of Regensburg, Universitatsstrasse 31, 93040 Regensburg, Germany

[3] Department of Systematics, Biodiversity and Evolution of Plants (with Herbarium), Albrecht-von-Haller-Institute, Georg-August-University Göttingen, Untere Karspuele 2, 37073 Göttingen, Germany

Published online: 17 October 2018

(sometimes called monotypic) endemic genera are of special interest due to the notion that their morphological uniqueness and geographical isolation may reflect the long-lasting phylogenetic independence of a palaeo-endemic or "living fossil" lineage. Following Gould (2002), living fossils are species or genera "belonging to ancient lineages from which most species are now extinct, and which have undergone relatively little evolutionary change" (Wright et al. 2012).

The flora of Greece is rich in flowering plant endemics, approximately 1462 taxa (1278 species and 452 subspecies from 270 genera and 58 families), and owes this richness in endemic taxa (22.2%) to small-scale differentiation and speciation processes in its mountain and island habitats. Additionally, Greece, as part of the Balkan Peninsula, has probably acted as a refuge for taxa of the surrounding floristic regions through geological times (Dimopoulos et al. 2013). Many of these plant endemics are considered to be neo-endemic species, which have probably formed in relatively recent times through speciation events, potentially driven by geological and climatological changes in the Pleistocene. However, the Greek flora also harbours seven endemic genera that may be palaeo-endemics or "living fossils". Six of these are unispecific (*Petromarula* R. Hedw., Campanulaceae; *Phitosia* Kamari & Greuter, Compositae; *Jancaea* Boiss., Gesneriaceae; *Lutzia* Gand., Brassicaceae; *Horstrissea* Greuter et al., and *Thamnosciadium* Hertvig, both Umbelliferae), and one (*Hymenonema* Cass., Compositae) comprises two species. For some of these genera, dated phylogenetic reconstructions are available, allowing classification as neo- or palaeo-endemics, but for others this information is still missing (i.e. *Horstrissea* and *Thamnosciadium*), or published conclusions have to be considered preliminary due to incomplete sampling in closely related genera (i.e. *Petromarula*, Cellinese et al. 2009; *Phitosia*, Enke and Gemeinholzer 2008; and *Hymenonema*, Tremetsberger et al. 2013).

The genus *Hymenonema* belongs to the tribe Cichorieae of the sunflower family (Compositae or Asteraceae) and comprises perennial herbs growing in stony places, cliffs, roadsides, and olive groves. Its two species, *H. laconicum* Boiss. & Heldr. and *H. graecum* (L.) DC., are found in the lowlands of the southern Peloponnisos mountains, and on most of the Kiklades islands and islets, respectively (Liveri et al. 2018). Phylogenetic reconstruction for the tribe based on nrDNA ITS sequences (Tremetsberger et al. 2013) indicated that the genus is a member of the subtribe Scolyminae, together with *Catananche* L. (5 spp.), *Gundelia* L. (6 spp.), and *Scolymus* L. (3 spp.). *Hymenonema* diverged from its sister genus *Scolymus* around 8.5 Ma ago, while the crown age of the whole subtribe was dated to 19.9 Ma (13.1–26.4 Ma). However, each of the four genera was represented only by a single species (i.e. *C. caerulea*, *G. tournefortii*, *H. graecum*, and *S. hispanicus*), which may have influenced the results, especially since the members of the subtribe exhibit a considerable range of life histories (annual, biennial, and perennial), which may affect dating due to very different generation times.

Owing to the incomplete taxonomic sampling of Tremetsberger et al. (2013) and the focus on *Hymenonema* in the present study, we aimed at a complete sampling of the three crown-group genera *Catananche*, *Hymenonema*, and *Scolymus.* Additionally, we enlarged the sampling of molecular sequence data by adding sequence information from the chloroplast genome and from a single-copy nuclear region. By this, we aim at a more conclusive phylogenetic reconstruction of relationships among the members of the subtribe and at a better supported dating of its differentiation processes, especially in terms of stem and crown ages of the genus *Hymenonema.* We further aim at a species tree-based reconstruction of the biogeographical history of the subtribe.

Materials and methods

Plant material

Individuals from most of the taxa belonging to subtribe Scolyminae and occurring in Greece (*Catananche lutea*, *Hymenonema graecum*, *H. laconicum*, *Scolymus hispanicus*), were collected during field excursion in 2013–2015. Herbarium specimens of all the collected taxa are lodged at the Herbarium of the University of Patras (UPA). For the molecular analysis, DNA extracts were obtained either from silica-gel-dried leaves of specimens collected in the wild or from herbarium specimens housed at UPA. For the rest of the taxa of the subtribe Scolyminae, DNA extracts were obtained from herbarium specimens from the Herbarium of the Botanic Garden and Botanical Museum Berlin-Dahlem (B; see Table 1 and Online Resource 1).

Since *Hymenonema* is the main focus of the present study, ten accessions belonging to this genus were included (six for *H. graecum* and four for *H. laconicum*). The remaining 21 accessions included 2–3 from each taxon of the subtribe (except for *Catananche montana* Coss. & Durieu for which only one was available). The genus *Gundelia* was used as an outgroup, with one accession from each of the two species. A total of 31 accessions were included in the present study.

DNA extraction, amplification, and sequencing

The samples were extracted using a modified protocol (Oberprieler et al. 2018) based on the CTAB method of Doyle and Doyle (1987). The quality of the extracted DNA was checked on 1.5% TBE agarose gel.

For the phylogenetic analyses, we amplified two intergenic spacer regions on the plastid genome (*trn*L-*trn*F and

Table 1 List of the samples used in the present study and their voucher information (for detailed information see Online Resource 1)

Taxon	Accession code	Location	Coordinates	Collector	Voucher	GenBank (*trn*L-*trn*F)	GenBank (*rpl*32-*trn*L)	GenBank ITS1/ITS2	GenBank *D10*
Catananche arenaria Coss. & Durieu	A146	Ma, Anti-Atlas, Tizi Mighert, 1050 m	29°21′N, 09°48′W	*Vogt 11885* and *Oberprieler 6333*	B 10 0550242	MH728955	MH728837	MH728893/MH728924	MH728868
	A862	Ma, Er-Rachidia, Er-Rachidia-Boudnib, 1110 m	31°55′N, 04°16′W	*Vogt 10400* and *Oberprieler 4848*	B 10 0209168	MH728963	MH728845	MH728901/MH728932	MH728875
	A894	Tn, Gafsa, Moulares, 400 m	34°27′N, 08°13′E	*Vogt 12739* and *Oberprieler 7044*	B 10 0209169	MH728970	MH728852	MH728908/MH728939	MH728881
Catananche caerulea L.	A868	Ma, Er-Rachidia, Tunnel du Legionaire	32°11′N, 04°21′W	*Vogt 5397*, *Bayón* and *Oberprieler*	B 10 0550629	MH728967	MH728849	MH728905/MH728936	MH728879
	A863	Hs, Huesca, Arro, 700 m	–	*Ern 4272* et al. (cult. in HB Berolinense)	B 10 0550626	MH728964	MH728846	MH728902/MH728933	MH728876
	A871	Tn, Kasserine, Djebel Chambi, 1530 m	35°12′N, 08°41′E	*Vogt 12607* and *Oberprieler*	B 10 0550628	MH728968	MH728850	MH728906/MH728937	MH728880
Catananche caespitosa Desf.	A149	Ma, Er-Rachidia, Tahout-ou-Fillali, 1910 m	32°40′N, 05°24′W	*Vogt 5859*, *Bayón* and *Oberprieler*	B 10 0550619	MH728957	MH728839	MH728895/MH728926	MH728870
	A864	Ma, Meknes, Col du Zad, 2100 m	33°02′N, 05°04′W	*Vogt 9446* and *Oberprieler 3884* [Iter Medit. V: no 18-0719]	B 10 0348475	MH728965	MH728847	MH728903/MH728934	MH728877
Catananche lutea L.	A910	Gr, Lakonia, Gerakas, 15 m	36°47′N, 23°04′E	*Liveri* and *Ketsilis-Rinis s.n.* [16.06.2014]	UPA	MH728985	MH728867	MH728923/MH728954	MH728892
	A147	Tn, El Kef, Kalaat Khasba, 880 m	35°42′N, 08°25′E	*Vogt 12516* and *Oberprieler 6821*	B 10 0550621	MH728956	MH728838	MH728894/MH728925	MH728869
	A865	Cy, Paphos, Peyia, 250–300 m	–	*Vogt 8716*	B 10 0550622	MH728966	MH728848	MH728904/MH728935	MH728878
Catananche montana Coss. & Durieu	A311	Ag, Bouira, Tikja, 1600 m	–	*Dubuis* and *Maurel s.n.* [01.07.1976]	B 10 0209165	MH728962	MH728844	MH728900/MH728931	MH728874
Gundelia aragatsii Vitek et al.	A900	Ar, Aragatsotn, Avtona-Kakavadzor, 1890 m	40°22′N, 44°02′E	*Vitek 06-1218*	B 10 0349291	MH728975	MH728857	MH728913/MH728944	
Gundelia tournefortii L.	A872	Cy, Giolou, 360 m	34°54′N, 32°29′E	*Hand 5796* and *Christodoulou*	B 10 0350430	MH728969	MH728851	MH728907/MH728938	

Table 1 (continued)

Taxon	Accession code	Location	Coordinates	Collector	Voucher	GenBank (*trn*L-*trn*F)	GenBank (*rpl32-trn*L)	GenBank ITS1/ITS2	GenBank *D10*
Hymenonema graecum (L.) DC.	A901	Gr, Naxos, Prokopios, 30 m	–	*Jäth s.n.* [29.09.1989]	B 10 0209163	MH728976	MH728858	MH728914/MH728945	MH728883
	A902	Gr, Tinos, Monastiri, Arnados, Dio Xoria, 350–450 m	37°33′N, 25°11′E	*Liveri* and *Ketsilis-Rinis 117*	UPA	MH728977	MH728859	MH728915/MH728946	MH728884
	A903	Gr, Andros, Batsi, 45 m	37°51′N, 24°47′E	*Liveri* and *Ketsilis-Rinis 115*	UPA	MH728978	MH728860	MH728916/MH728947	MH728885
	A904	Gr, Kithnos, Merichas Bay, 20–40 m	37°23′N, 24°23′E	*Liveri* and *Ketsilis-Rinis 100*	UPA	MH728979	MH728861	MH728917/MH728948	MH728886
	A905	Gr, Siros, Kini	37°26′N, 24°57′E	*Liveri* and *Ketsilis-Rinis 107*	UPA	MH728980	MH728862	MH728918/MH728949	MH728887
	A256	Gr, Serifos, Koutalas, 400 m	–	*Malicky s.n.* [13.05.1990]	W	MH728961	MH728843	MH728899/MH728930	
Hymenonema laconicum Boiss. & Heldr.	A906	Gr, Lakonia, Lagkada gorge, 800 m	37°05′N, 22°19′E	*Kyriakopoulos 1524*	UPA	MH728981	MH728863	MH728919/MH728950	MH728888*
	A907	Gr, Lakonia, Geraki, Alepohori, 300–400 m	36°59′N, 22°44′E	*Liveri* and *Ketsilis-Rinis 124*	UPA	MH728982	MH728864	MH728920/MH728951	MH728889
	A908	Gr, Arkadia, Leonidio-Tsitalia, 113 m	37°09′N, 22°53′E	*Kofinas* and *Dolianitis 129*	UPA	MH728983	MH728865	MH728921/MH728952	MH728890
	A909	Gr, Lakonia, Krokees, 350 m	36°53′N, 22°32′E	*Liveri* and *Kofinas 131*	UPA	MH728984	MH728866	MH728922/MH728953	MH728891
Scolymus grandiflorus Desf.	A152	Ma, Melilla, Segangane-Aazanèn, 190 m	35°10′N, 03°04′W	*Vogt 10907* and *Oberprieler 5355*	B 10 0158439	MH728960	MH728842	MH728898/MH728929	MH728873*
	A896	Ma, Oujda, Tizi-n-Tirchete, 910 m	34°50′N, 02°08′W	*Vogt 15291* and *Oberprieler 9600*	B 10 0158440	MH728971	MH728853	MH728909/MH728940	
Scolymus hispanicus L.	A898	Gr, Lakonia, Velies, 100–120 m	36°43′N, 22°58′E	*Liveri* and *Ketsilis-Rinis s.n.* [15.06.2014]	UPA	MH728973	MH728855	MH728911/MH728942	
	A897	Ma, Marrakech, El-Kelaa-Srarhna, 410 m	32°09′N, 07°06′W	*Vogt 5770*, *Bayón* and *Oberprieler*	B 10 0550616	MH728972	MH728854	MH728910/MH728941	
	A150	Tn, Siliana, Makthar, 910 m	35°47′N, 09°13′E	*Vogt 13467* and *Oberprieler 7772*	B 10 0550243	MH728958	MH728840	MH728896/MH728927	MH728871*

Table 1 (continued)

Taxon	Accession code	Location	Coordinates	Collector	Voucher	GenBank (*trn*L-*trn*F)	GenBank (*rpl*32-*trn*L)	GenBank ITS1/ITS2	GenBank *D10*
Scolymus maculatus L.	A899	Ma, Sefiane, Col de Rmel, 140 m	34°47′N, 05°45′W	*Vogt 9617* and *Oberprieler 4053* [= Iter Medit. V: no 54-1795]	B 10 0550617	MH728974	MH728856	MH728912/MH728943	MH728882
	A151	Hs, Cádiz, Tarifa, 1–5 m	–	*Vogt 9276* and *Prem-Vogt*	B 10 0550244	MH728959	MH728841	MH728897/MH728928	MH728872

Vouchers are housed in the herbaria of the Botanic Garden and Botanical Museum Berlin-Dahlem (B; with herbarium accession numbers indicated) and of the University of Patras (UPA). Asterisks (*) besides GenBank accession numbers indicate samples cloned for marker *D10*

*rpl*32-*trn*L), the nuclear ribosomal internal transcribed spacer region (nrDNA ITS) and one single-copy nuclear marker (*D10*), selected from those characterised by Chapman et al. (2007) for the sunflower family. The screening of the Chapman et al. (2007) markers was done with two *Catananche* species (*C. arenaria*, *C. caerulea*) and comprised 28 different markers; eight primer combinations resulted in sequenceable PCR products, of which one (*D10*) was readable and variable. The plastid spacer *trn*L*(UAA)*-*trn*F*(GAA)* was amplified using the primers [trnL]e and [trnF]f (Taberlet et al. 1991), whereas the primers trnL$^{(UAG)}$ and rpl32-F (Shaw et al. 2007) were used to amplify *rpl*32-*trn*L. PCR amplification was performed using the Taq DNA Polymerase Master Mix Red in a final volume of 12.5 µl, using the protocol suggested by the company (Ampliqon, Odense, Denmark). Except for a few cases, the following thermal profile was employed for all amplifications: 2 min at 95 °C, then 35 cycles of 30 s at 95 °C, 30 s at the annealing temperature, 30 s at 72 °C, and a final extension of 5 min at 72 °C. The annealing temperatures were 50 °C for the *trn*L-*trn*F and 58 °C for the *rpl*32-*trn*L amplifications.

The nrDNA ITS1 and ITS2 spacers were amplified separately using primers P1 and P2 (White et al. 1990) for ITS1, and P3 and P4 (White et al. 1990) for ITS2. For one accession of the species *Catananche caespitosa* (A864), different primers [18SF (Rydin et al. 2004) and P2B (White et al. 1990) for ITS1, and P3 (White et al. 1990) and SR (Blattner et al. 2001) for ITS2] were used, because no bands were obtained using the standard primers. The annealing temperature for the ITS reactions was 50 °C. The annealing temperature for the single-copy nuclear marker (*D10*) using primers D10f and D10r (Chapman et al. 2007) was 60 °C or 62 °C. Six accessions (see Table 1) needed to be cloned for the single-copy nuclear marker *D10* due to illegible electropherograms in direct sequencing. Cloning was done using the CloneJET PCR cloning kit (Fisher Scientific, Waltham, Massachusetts, USA) according to the manufacturer's recommendations. Eight colonies were picked for each cloned accession, and three of them were sequenced. Finally, a single sequence per accession (i.e. the sequence most similar to the sequences of other, directly sequenced accessions) was included in the alignment and in the subsequent phylogenetic analyses, assuming that more dissimilar sequences resulted from co-amplification of paralogous loci.

The PCR products were purified using Agencourt AMPure magnetic beads (Agencourt Bioscience Corporation, Beverly, Massachusetts, USA). Cycle sequencing was performed by Macrogen (Seoul, Korea) using amplification primers. The obtained electropherograms were carefully checked for ambiguities using Chromas Lite v.2.10 (Technelysium Pty Ltd., Tewantin, Australia; http://technelysium.com.au/chromas.html).

Data processing and gene tree reconstruction

Alignments were prepared using the Clustal W progressive method for multiple sequences alignment (Thompson et al. 1994) on the internet platform: http://www.ebi.ac.uk/Tools/msa/clustalw2/. Final alignments (see Online Resources 2-6) were checked and edited manually with BioEdit v.7.2.5 (http://www.mbio.ncsu.edu/bioedit/bioedit.html) for cases of obvious alignment errors (i.e. non-homologous gap formations that could be interpreted as homologous ones without being less parsimonious). Gaps were coded as binary characters using the simple gap coding method of Simmons and Ochoterena (2000) as implemented in the software GapCoder (Young and Healy 2003).

Maximum parsimony (MP) analysis was done for the plastid markers (*trn*L-*trn*F and *rpl*32-*trn*L concatenated into a single alignment), nrDNA ITS, and *D10* separately, using PAUP* 4.0 v.b10 (Swofford 2002) and implementing a branch-and-bound search with MulTrees option in action. Support for clades was evaluated using the parsimony bootstrap (Felsenstein 1985). For the nrDNA ITS and the *D10* data set, 100 bootstrap replicates with a branch-and-bound search were performed. For the cpDNA markers, a heuristic search was used for the bootstrap replicates with 100 random addition sequence replicates per bootstrap replicate (again 100 bootstrap replicates) and a single tree held at each step during stepwise addition and the TBR option in action.

Bayesian inference (BI) phylogenetic analyses were performed for the plastid markers, nrDNA ITS, and *D10* separately, as for the MP analyses, using the software MrBayes v.3.2.1 (Ronquist and Huelsenbeck 2003). The model that best fit the sequence information for each of the different markers was selected based on the Akaike Information Criterion (AIC) in jModelTest v.2.1.6. (Darriba et al. 2015) and is shown in Table 2. The BI analyses were conducted using seven heated chains and one cold one, with a chain heating parameter of 0.2 in the two parallel runs. The Metropolis-coupled Markov chain Monte Carlo (MC^3) chains were run for 5×10^6 generations, with trees sampled every 1000th generation. Attainment of convergence among searches was checked by examining the average standard deviation of split frequencies as reported by MrBayes and by comparing likelihood values and parameter estimates in Tracer v.1.6 (Rambaut and Drummond 2007). Convergence of runs was assumed when values for the average standard deviation of split frequencies bumped below 0.01 and effective sample size (ESS) values for all parameters was higher than 100. A burn-in of 25% of the run length was applied as by default (Ronquist et al. 2011), having checked that convergence between runs was reached well before that generation number. The remaining trees were summarised using the "halfcompat" setting (equivalent to a 50% majority rule) for the consensus tree.

Species tree inference and molecular dating

In order to infer a total-evidence species tree based on all markers and accessions, we submitted the complete data set to the species tree reconstruction and divergence time estimation procedure in the program *BEAST (Heled and Drummond 2010). Therefore, the species tree reconstruction did not follow a traditional concatenation method of phylogeny reconstruction from multiple gene regions, but rather a multi-species coalescent model that uses the separate gene trees to infer a global species tree based on coalescent theory (coalescence of gene tree lineages within species lineages). This model assumes no gene flow between lineages once speciation has occurred and requires the a priori assignment of individual sequences to the species defined. The BEAST.xml input files were produced using BEAUti v.1.8.1 (Drummond et al. 2012) and comprised ten different partitions: the sequence information plus the binary coded gap information for each of the five markers. (The two plastid regions as well as the three nuclear ones were imported separately, although tree and clock models were kept linked for each sequence and its corresponding indel partition.) Nucleotide substitution models were chosen according to jModelTest v.2.1.6. (Darriba et al. 2015), but model parameters were allowed to vary in parameter space around a mean value corresponding to the one given by jModelTest assuming a

Table 2 Aligned lengths, substitution models (with model parameters), and number of variable and parsimony-informative sites (PI; calculated in PAUP*, Swofford 2002) for each molecular region

Marker	Length	Variable sites	PI variable sites	Model	Model parameters			Coded indels
					Base frequencies (A, C, G, T)	Substitution rates (A–C, A–G, A–T, C–G, C–T, G–T)	Gamma distribution shape parameter	
cpDNA	1531	241 (16%)	177 (12%)	TVM + G	0.36, 0.14, 0.15, 0.35	1.0, 1.0, 0.1, 1.2, 1.0, 1.0	1.0671	78
nrDNA ITS	570	155 (38%)	135 (33%)	GTR + G	0.22, 0.27, 0.27, 0.24	0.7, 1.2, 0.8, 0.2, 3.6, 1.0	0.6551	26
D10	411	262 (46%)	209 (37%)	HKY + I+G	0.32, 0.19, 0.19, 0.29	1.2, 2.5, 0.9, 1.2, 2.7, 1.0	0.6511	43

normal distribution (Table 2). For the five indel partitions, the binary simple model was chosen.

In order to choose the best clock and species tree models, we performed different analyses using the "strict clock" or the "log-normal relaxed clock" (Drummond et al. 2006), and with the "Yule" (Yule 1924) or the "Birth–Death" (Kendall 1948) models as species tree priors. The best models were selected by calculating the marginal likelihood estimates (MLE) using stepping-stone sampling (SS; Xie et al. 2011; chain length for the MLE = 10^6, number of steps = 100 and alpha = 0.3) in BEAST v.1.8.1 (Drummond et al. 2012). Since from preliminary analyses the position of *Gundelia* was uncertain, we also ran different sets of analyses with and without enforcing the outgroup position of the above-mentioned genus. Concerning the population size model, the pairwise linear model with constant root was applied in all analyses. The analyses were run in the CIPRES Science Gateway https://www.phylo.org/portal2/ for 10^9 generations, sampling every 50,000th generation. Once the best models were found (Table 3), two independent runs were performed, and—after checking convergence and determining burn-in values in Tracer v.1.6 (ESS values higher than 200 were considered acceptable)—the results of the two analyses were merged using LogCombiner v.1.8.1 (Drummond et al. 2012) and applying a burn-in period of 10% of the total number of trees sampled. Finally, the remaining 18,000 trees were used to construct a maximum clade credibility tree with a posterior probability limit set to 0.5 using TreeAnnotator v.1.8.1 (Drummond et al. 2012).

In order to obtain absolute divergence times, we used the age estimation of the subtribe Scolyminae given by Tremetsberger et al. (2013) to calibrate our species tree reconstruction. In this study, the authors estimated the minimum ages of the most recent common ancestor of the tribe Cichorieae and its subtribes, based on nrDNA ITS sequence and using the oldest fossils of *Cichorium*-, *Scorzonera*- and *Sonchus*-type pollen as calibration points. Since different reconstructions were presented in Tremetsberger et al. (2013)—with constrained and unconstrained topology, and calibrating stem or crown groups—we used the broadest interval among different age estimates to calibrate the crown age of the Scolyminae. With this interval ranging from 13.1 to 32.5 Ma, we applied a normally distributed *tmrca* prior (mean: 22.8 Ma, SD: 5.9) to calibrate the root of our species tree reconstruction.

Table 3 Means and 95% confidence intervals of marginal likelihood estimates from 10 replicate analyses under different clock and species tree models

	Yule	Birth–death
Strict clock		
Enforced topology	−8579.212 (±2.22)	−8576.899 (±2.66)
Unenforced topology	−8581.341 (±2.84)	−8581.442 (±2.52)
Relaxed clock		
Enforced topology	−8542.904 (±1.3)	−8542.327 (±2.07)
Unenforced topology	−8550.245 (±1.69)	**−8539.960 (±2.57)**

The bold likelihood value indicates the combination of priors that best fits the data

Biogeographical analysis

Dispersal, vicariance, and extinction events in the phylogeny of Scolyminae were inferred by maximum likelihood-based ancestral area reconstruction implemented in Lagrange v20130526 (Ree and Smith 2008). The analyses were run under Python v2.7.13 (with the two libraries *scipy* and *numpy* installed) and a script prepared with the online Lagrange configurator (http://reelab.net/lagrange/configurator/index). The calibrated, ultrametric species tree was used as input, and species distributions were determined based on information from the Euro + Med plantbase (2006–2017). The six areas used in the biogeographical analysis were defined on the basis of three criteria: (1) geographical boundaries that may have acted as barriers to dispersal (e.g. water bodies and mountain ranges); (2) congruent distributional ranges of endemic species of the study group (e.g. A, *Hymenonema* spp.; B, *Gundelia* spp.; C, *Catananche areanaria*, *C. caespitosa*, and *C. montana*); and (3) congruent distributional ranges (sympatric distribution) shared by two or more species based on their Euro + Med plantbase distribution information (Fig. 1). A single adjacency matrix was specified for the analysis (Table 4a), assigning a dispersal rate of 1.0 between adjacent areas and 0.1 between non-adjacent areas as done in a comparable biogeographical analysis by Tremetsberger et al. (2016). No restriction concerning the number of ancestral areas allowed was enforced.

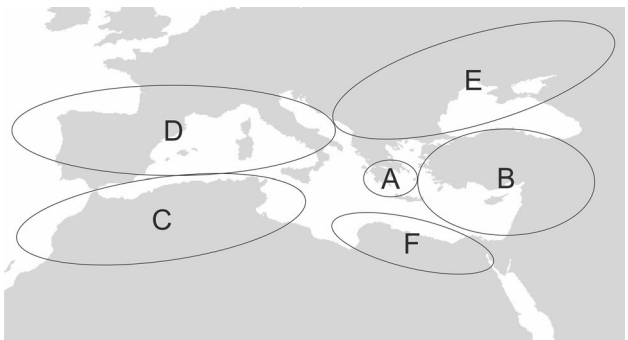

Fig. 1 Areas used in the biogeographical Lagrange analysis. A, Greece; B, E Mediterranean, S Caucasus; C, NW Africa; D, SW Europe; E, Balkans, N Caucasus; F, NE Africa. (Base map modified from a freely distributed global map of the world downloaded from http://www.diva-gis.org/Data.htm)

Table 4 Model-based ancestral area reconstruction in the *Scolyminae* using the software Lagrange (Ree and Smith 2008)

(a)

Areas	
A	Greece
B	E Mediterranean, S Caucasus
C	NW Africa
D	SW Europe
E	Balkans, N Caucasus
F	NE Africa

	A	B	C	D	E	F
A	–	Adjacent	Non-adjacent	Adjacent	Adjacent	Non-adjacent
B		–	Non-adjacent	Non-adjacent	Adjacent	Adjacent
C			–	Adjacent	Non-adjacent	Adjacent
D				–	Adjacent	Non-adjacent
E					–	Non-adjacent

(b)

Node	Split	ln *L*	Rel. prob.
1	[A|A]	− 38.8	0.04657
	[D|D]	− 39.32	0.02754
	[ABCDF|B]	− 39.33	0.02726
	[ABCD|B]	− 39.37	0.02637
	[ABCDEF|B]	− 39.51	0.0229
2	[D|D]	− 38.54	0.06045
	[A|A]	− 38.56	0.05884
	[C|ABCDEF]	− 38.87	0.04345
	[D|ABCDEF]	− 39.03	0.03694
	[C|C]	− 39.24	0.02977
3	[A|ABCDEF]	− 37.4	0.1881
	[A|ABCD]	− 38.07	0.09669
	[A|ABCDF]	− 38.14	0.08962
	[A|ACD]	− 38.37	0.07116
	[A|ABD]	− 38.55	0.05977
4	[C|ACD]	− 37.09	0.2567
	[C|ABCD]	− 37.22	0.2247
	[C|C]	− 37.89	0.1157
	[C|CD]	− 38.23	0.08225
	[C|ABD]	− 38.24	0.08117
5	[C|C]	− 35.82	0.9129
	[C|CD]	− 39.0	0.03807
6	[D|ABCDEF]	− 37.31	0.2063
	[A|ABCDEF]	− 37.33	0.2025
	[C|ABCDEF]	− 38.3	0.07672
	[D|ABCDF]	− 38.41	0.06836
	[B|ABCDEF]	− 38.42	0.06796
7	[ABCD|C]	− 36.8	0.3432
	[ACD|C]	− 37.18	0.2346
	[ABD|C]	− 37.78	0.1288
	[C|C]	− 38.34	0.07372
	[CD|C]	− 38.4	0.06949

Table 4 (continued)

(b)

Node	Split	ln *L*	Rel. prob.
8	[C|C]	−35.95	0.8014
	[CD|C]	−37.66	0.1457
	[D|C]	−39.29	0.02847
9	[A|A]	−35.82	0.9124
	[AE|A]	−40.09	0.01281
	[A|AE]	−40.09	0.01281
	[AD|A]	−40.18	0.01162
	[A|AD]	−40.18	0.01162
10	[C|ABCDEF]	−36.68	0.3852
	[D|ABCDEF]	−36.74	0.3628
	[C|ABCDF]	−38.24	0.08128
	[D|ABCDF]	−38.3	0.07656
	[C|ABCD]	−39.2	0.03104
11	[B|B]	−35.79	0.9413
	[BF|B]	−40.4	0.009386

(a) Areas and area adjacency matrix used as input. (b) Splits with associated log likelihoods (ln *L*) and relative probabilities (Rel. Prob.) for each node. Node numbers refer to those indicated in Fig. 3. Reconstructions are listed from the highest to the lowest relative probability; however, only the first five reconstructions per node are shown, except for those where the second reconstruction has a much lower relative probability

Results

Gene trees

The three gene trees with support values obtained both from the BI and MP analyses are shown in Fig. 2, and detailed information on the different regions used in the analyses is given in Table 2. In both the cpDNA (Fig. 2a) and nrDNA ITS (Fig. 2b) trees, the accessions of all three ingroup genera (*Hymenonema*, *Catananche*, and *Scolymus*) form monophyletic groups with strong posterior probability (PP) and/or bootstrap (BS) support. In the *D10* tree (Fig. 2c), *Hymenonema* and *Catananche* are recovered as monophyletic, but *Scolymus* lacks support as a monophyletic lineage and is instead recovered as a grade. In all three trees, *Scolymus* is the sister genus to *Hymenonema*. The reciprocal monophyly of the two species of *Hymenonema* is supported in the ITS tree, but not in the plastid or the *D10* tree; in the former, one accession of *H. graecum* is unresolved outside the *H. graecum* clade, while in the latter, one accession of *H. laconicum* is sister to a clade (*H. laconicum* + *H. graecum*).

Species tree and biogeographical analysis

The maximum clade credibility (MCC) tree obtained from the *BEAST analysis is shown in Fig. 3. The clock model that performed better was the log-normal relaxed clock, while the Birth–Death tree model outperformed the Yule model. Enforcing *Gundelia* as outgroup did not produce better results; therefore, the final analyses were performed with a relaxed clock, Birth–Death speciation model and unenforced topology (see Table 3 for information on the log marginal likelihood estimates and ranges obtained for all different models).

In the species tree obtained, the four genera of the subtribe Scolyminae are all monophyletic and receive high PP support values. While *Scolymus* is supported as sister to *Hymenonema*, with the time of divergence between the two genera estimated as 9.2 Ma ago (3.7–15.7 Ma), the relationships among *Gundelia*, *Catananche*, and the *Hymenonema–Scolymus* clade remain unresolved due to the lack of support for a sister-group relationship of the latter two lineages. Speciation within *Hymenonema* is inferred to have taken place in the Pleistocene, at around 1.3 Ma ago (0.4–2.3 Ma).

Model-based ancestral area reconstruction (Fig. 3, Table 4b) was equivocal for many of the ancestral nodes, due to both the uncertainties connected with the relationships among the major lineages in the species tree (see above) and likelihood values for many nodes supporting alternative vicariance scenarios (Table 4b). While we observed strong support for the differentiation of *Hymenonema* in Greece (node 9, area A), *Gundelia* in the E Mediterranean-S Caucasus region (node 11, area B), and the clade of *Catananche arenaria*, *C. caerulea*, and *C. caespitosa* in NW Africa (nodes 5 and 8, area C), all other nodes of the underlying species tree received at least two biogeographical scenarios with nearly equivalent likelihoods. For the most basal nodes

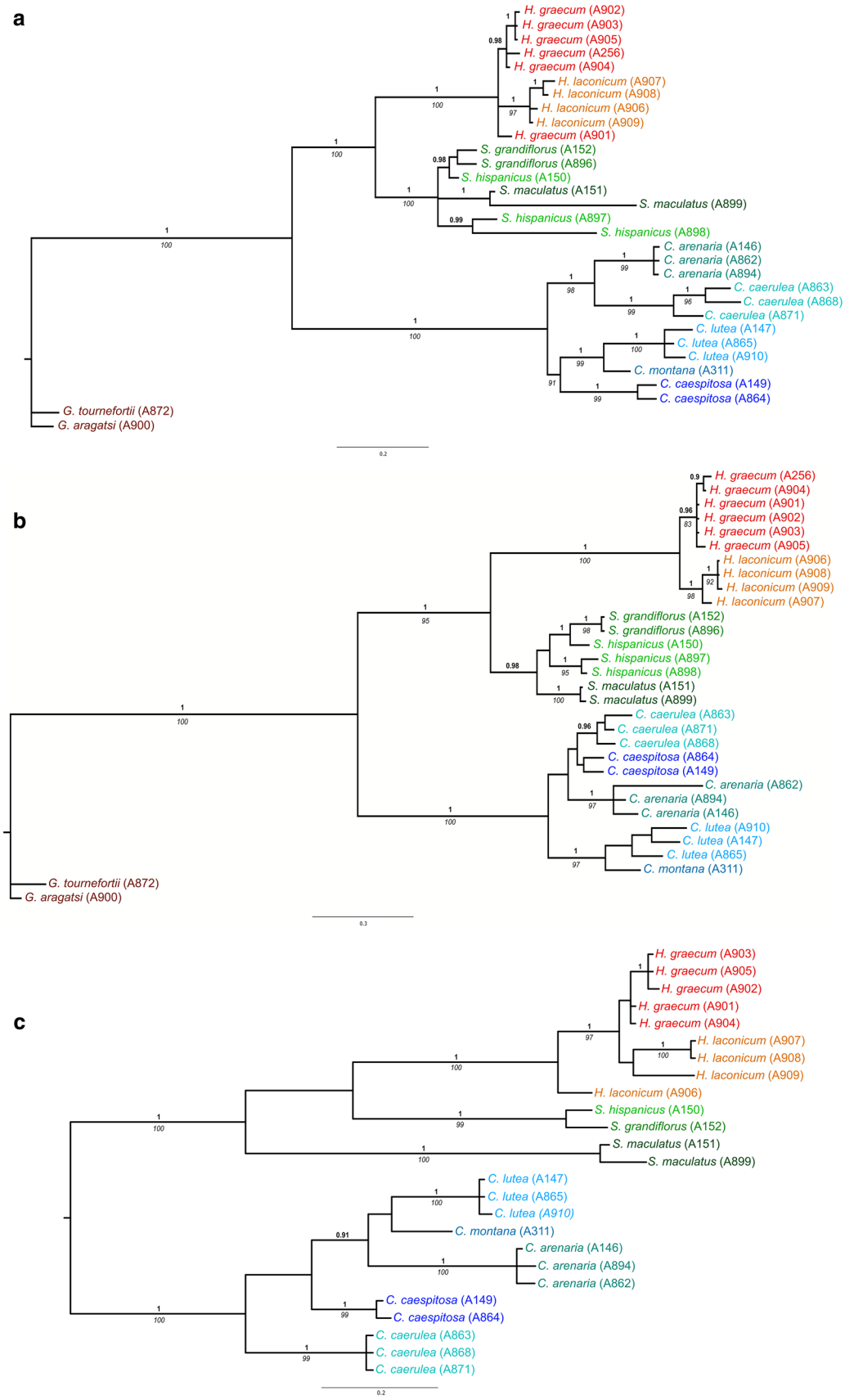
a
H. graecum (A902)
H. graecum (A903)
H. graecum (A905)
H. graecum (A256)
H. graecum (A904)
H. laconicum (A907)
H. laconicum (A908)
H. laconicum (A906)
H. laconicum (A909)
H. graecum (A901)
S. grandiflorus (A152)
S. grandiflorus (A896)
S. hispanicus (A150)
S. maculatus (A151)
S. maculatus (A899)
S. hispanicus (A897)
S. hispanicus (A898)
C. arenaria (A146)
C. arenaria (A862)
C. arenaria (A894)
C. caerulea (A863)
C. caerulea (A868)
C. caerulea (A871)
C. lutea (A147)
C. lutea (A865)
C. lutea (A910)
C. montana (A311)
C. caespitosa (A149)
C. caespitosa (A864)
G. tournefortii (A872)
G. aragatsi (A900)
0.2
b
H. graecum (A256)
H. graecum (A904)
H. graecum (A901)
H. graecum (A902)
H. graecum (A903)
H. graecum (A905)
H. laconicum (A906)
H. laconicum (A908)
H. laconicum (A909)
H. laconicum (A907)
S. grandiflorus (A152)
S. grandiflorus (A896)
S. hispanicus (A150)
S. hispanicus (A897)
S. hispanicus (A898)
S. maculatus (A151)
S. maculatus (A899)
C. caerulea (A863)
C. caerulea (A871)
C. caerulea (A868)
C. caespitosa (A864)
C. caespitosa (A149)
C. arenaria (A862)
C. arenaria (A894)
C. arenaria (A146)
C. lutea (A910)
C. lutea (A147)
C. lutea (A865)
C. montana (A311)
G. tournefortii (A872)
G. aragatsi (A900)
0.3
c
H. graecum (A903)
H. graecum (A905)
H. graecum (A902)
H. graecum (A901)
H. graecum (A904)
H. laconicum (A907)
H. laconicum (A908)
H. laconicum (A909)
H. laconicum (A906)
S. hispanicus (A150)
S. grandiflorus (A152)
S. maculatus (A151)
S. maculatus (A899)
C. lutea (A147)
C. lutea (A865)
C. lutea (A910)
C. montana (A311)
C. arenaria (A146)
C. arenaria (A894)
C. arenaria (A862)
C. caespitosa (A149)
C. caespitosa (A864)
C. caerulea (A863)
C. caerulea (A868)
C. caerulea (A871)
0.2

◂**Fig. 2** 50%-majority-rule Bayesian consensus trees of **a** the concatenated data set of the two plastid intergenic spacer regions *trn*L-*trn*F and *rpl*32-*trn*L, **b** the nrDNA ITS region and **c** the single-copy nuclear region *D10*. Numbers above branches indicate Bayesian posterior probabilities, while those below the branches refer to the bootstrap support values from the maximum parsimony (MP) analyses. Accession codes (see Table 1) are given in brackets in the leaf labels

of the tree (nodes 1 and 2), however, differentiation on the Eurasian platform (areas A and D: Greece and SW Europe) for the pre-Messinian Miocene (i.e. ~ 20–5.3 Ma) appears reasonable when taking into account also reconstructions with suboptimal likelihood values. Additionally, the present reconstructions also point towards the differentiation of *Scolymus* in connection with the dispersal of this lineage throughout the whole Mediterranean region (node 3), of *Catananche* in connection with the dispersal into NW Africa (node 4), and of *Gundelia* in connection with dispersal into the E Mediterranean-S Caucasus region (node 11) (Fig. 3).

Discussion

The present analysis provides further support for the finding of Kilian et al. (2009) and Tremetsberger et al. (2013) of the sister-group relationship between *Hymenonema* and *Scolymus*, and for *Catananche* and *Gundelia* being more distantly related. With its crown age inferred at 20.8 Ma (11.3–29.9 Ma), our age estimates are consistent with the hypothesis that the subtribe is composed of a group of old lineages with long-term isolation. This circumstance may explain the considerable morphological and life-history diversity exhibited by its members, with scapose, annual to perennial herbs in *Catananche* and *Hymenonema*, herbs with long and spiny stems in *Scolymus*, and plants with single-flowered capitula aggregated into capitulate syncalathia in *Gundelia.*

In contrast to the high stem ages of the four genera of Scolyminae (9.2–20.8 Ma) dating back to their differentiation in the Early and Middle Miocene, their crown ages point to much more recent diversification into the present-day species during the Pliocene (*Catanache*, *Scolymus*) or even during the Pleistocene (*Hymenonema*, *Gundelia*). As far as *Hymenonema* is concerned, its stem age of 9.2 Ma (3.7–15.7 Ma) places it at an intermediate age among the Greek palaeoendemic genera, with the Cretan endemic *Petromarula* (Campanulaceae) showing phylogenetic independence for the last 20–25 Ma (Cellinese et al. 2009), on the one hand, and the possibly much younger *Jancaea* (Gesneriaceae) on the other (< 7.5 Ma; Petrova et al. 2015). The third endemic genus of Greece, for which a date of origin is available, the unispecific genus *Phitosia* (Compositae), belongs to another subtribe of Cichorieae (Chondrillinae) but shows a stem age comparable with that of *Hymenonema* (i.e. 12.4 Ma; Tremetsberger et al. 2013). The highly dynamic and complex Tertiary history of the Northern Peri-Tethys platform with its recurrent episodes of palaeogeographic reorganisation and basin rearrangements (Meulenkamp and Sissingh 2003) may have triggered the differentiation processes among the four

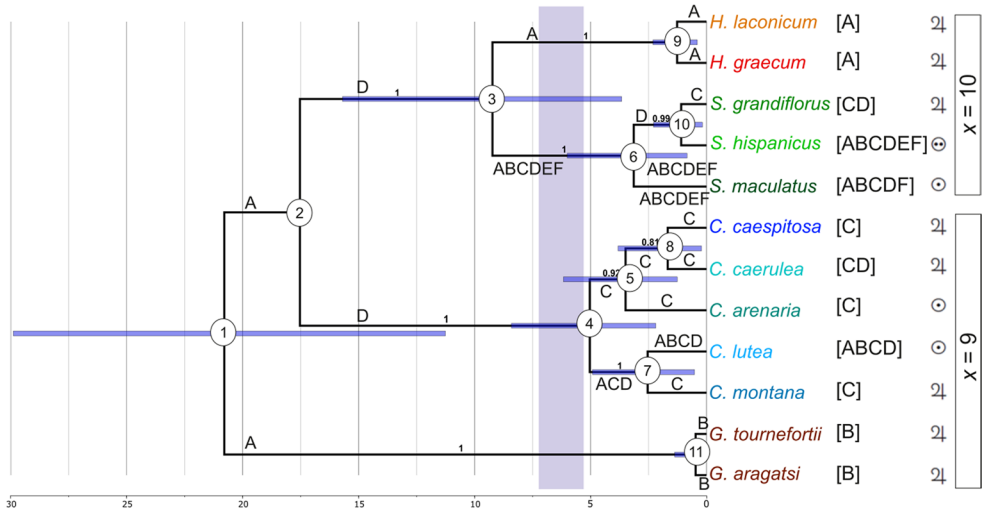

Fig. 3 Dated species tree for the subtribe Scolyminae estimated using *BEAST, based on sequence data from four regions (*trn*L-*trn*F, *rpl*32-*trn*L, nrDNA ITS, *D10*). The error bars indicate the 95% highest posterior density intervals for the divergence times estimates. Numbers above branches indicate Bayesian posterior probabilities from the species tree analysis under the multi-species coalescent model. Base chromosome numbers and growth forms (i.e. ♃ : perennial; ☉ : annual; ⚇ : biennial) are indicated to the right of the taxon names. The ancestral areas with the highest single relative probability from Lagrange analysis are indicated with letters (A, Greece; B, E Mediterranean, S Caucasus; C, NW Africa; D, SW Europe; E, Balkans, N Caucasus; F, NE Africa)

generic lineages of Scolyminae on the Eurasian platform as inferred in our present maximum likelihood-based ancestral area reconstruction and may account for their long-lasting geographical isolation.

Contrary to its old stem age, the crown age of *Hymenonema* (i.e. 1.3 Ma; 0.4–2.3 Ma)—hence the separation of its two allopatrically distributed species *H. graecum* and *H. laconicum*—is very recent and falls into the Pleistocene. Since the Kiklades islands (home of *H. graecum*) and the Peloponnisos (*H. laconicum*) were connected through mainland Greece until the end of the Pliocene (c. 2 Ma; Fattorini 2002; Chatzimanolis et al. 2003), but subsequent eustatic sea-level changes during the Pleistocene were never severe enough to reconnect the Kiklades to mainland Greece (Greuter 1979; Comes et al. 2008; Poulakakis et al. 2015), this makes the Pliocene/Pleistocene boundary the most probable geological period for this allopatric speciation event. Similar examples of such allopatric speciation events are reported for the species pair *Symphytum creticum* (Willd.) Greuter & Rech.f. and *S. insulare* (Pawł.) Greuter & Burdet (as *Procopiana* Guşul., Greuter 1979) and between the subspecies *Centaurea laconica* Boiss. subsp. *laconica* and *C. laconica* Boiss. subsp. *lineariloba* (Halácsy & Dörfl.) E.Gamal-Eldin & Wagenitz (D. Phitos personal comm.). Morphological variation observed in *H. graecum* with even some populations on the Kiklades islands of Mikonos, Naxos, Siros, and Tinos showing character expressions intermediate between *H. graecum* and *H. laconicum* (Liveri et al. 2018) may constitute retained plesiomorphies from the joint ancestor and shows that allopatric differentiation processes through genetic drift and/or selection in the island populations of the former species may still be in full swing.

The present study elucidates the phylogenetic relationships of *Hymenonema* with its closest relatives, estimates the divergence time of the two species, and gives insight into the differentiation events that took place between its members. The separation of the two species falling into the Pleistocene and their geographical distribution (Liveri et al. 2018) strongly support the scenario of allopatric speciation and confirm an old line of isolation between Peloponnisos and Kiklades. The presence of morphologically intermediate plants between the two *Hymenonema* species that have been described recently (Liveri et al. 2018) reveals the possibility of a complex geographical speciation event in the Aegean Archipelago that could explain the lack of reciprocal monophyly in all surveyed markers. More collections of *H. graecum* from the Kiklades in a follow-up project and the utilisation of a higher number of molecular markers through the application of next-generation sequencing (NGS) methods like RAD-Seq or genotyping-by-sequencing (GBS) will probably help to discriminate between allopatric or peripatric speciation scenarios.

Acknowledgements This research was supported by an Erasmus + for Traineeships Grant to E.L. in 2014–2015. The suggestions by two anonymous reviewers improved the present contribution considerably and are thankfully acknowledged.

Compliance with ethical standards

Conflict of interest The authors declare no conflict of interests.

Information on Electronic Supplementary Material

Online Resource 1. List of the samples used in the present study and their voucher information. Asterisks (*) beside accession numbers indicate samples cloned for marker D10.
Online Resource 2. Alignment of the cpDNA *trn*L-*trn*F intergenic spacer region in FASTA format.
Online Resource 3. Alignment of the cpDNA *rpl*32-*trn*L intergenic spacer region in FASTA format.
Online Resource 4. Alignment of the nrDNA ITS1 region in FASTA format.
Online Resource 5. Alignment of the nrDNA ITS2 region in FASTA format.
Online Resource 6. Alignment of the nuclear single-copy region *D10* in FASTA format.

References

Blattner FR, Weising K, Bänfer G, Maschwitz U, Fiala B (2001) Molecular analysis of phylogenetic relationships among myrmecophytic *Macaranga* species (Euphorbiaceae). Molec Phylogen Evol 19:331–344. https://doi.org/10.1006/mpev.2001.0941

Cellinese N, Smith SA, Edwards EJ, Kim ST, Haberle RC, Avramakis M, Donoghue MJ (2009) Historical biogeography of the endemic Campanulaceae of Crete. J Biogeogr 36:1253–1269. https://doi.org/10.1111/j.1365-2699.2008.02077.x

Chapman MA, Chang J, Weisman D, Kesseli RV, Burke JM (2007) Universal markers for comparative mapping and phylogenetic analysis in the Asteraceae (Compositae). Theor Appl Genet 115:747–755. https://doi.org/10.1007/s00122-007-0605-2

Chatzimanolis S, Trichas A, Giokas S, Mylonas M (2003) Phylogenetic analysis and biogeography of Aegean taxa of the genus *Dendarus* (Coleaoptera: Tenebrionidae). Insect Syst Evol 34:3. https://doi.org/10.1163/187631203788964773

Comes HP, Tribsch A, Bittkau C (2008) Plant speciation in continental island floras as exemplified by *Nigella* in the Aegean archipelago. Philos Trans Roy Soc London B Biol Sci 363:3083–3096. https://doi.org/10.1098/rstb.2008.0063

Darriba D, Taboada GL, Doallo R, Posada D (2015) jModelTest 2: more models, new heuristics and parallel computing. Nat Meth 9:772. https://doi.org/10.1038/nmeth.2109

Dimopoulos P, Raus T, Bergmeier E, Constantinidis T, Iatrou G, Kokkini S, Strid A, Tzanoudakis D (2013) Vascular plants of Greece. An annotated checklist (Englera 31). Botanischer Garten und Botanisches Museum Berlin-Dahlem, Hellenic Botanical Society, Berlin, Athens

Doyle JJ, Doyle JL (1987) A rapid DNA isolation procedure for small quantities of fresh leaf tissue. Phytochem Bull 19:11–15. https://doi.org/10.1038/nmeth.2109

Drummond AJ, Ho SYW, Phillips MJ, Rambaut A (2006) Relaxed phylogenetics and dating with confidence. PLoS Biol 4:e88. https://doi.org/10.1371/journal.pbio.0040088

Drummond AJ, Suchard MA, Xie D, Rambaut A (2012) Bayesian phylogenetics with BEAUti and the BEAST 1.7. Molec Biol Evol 29:1969–1973. https://doi.org/10.1093/molbev/mss075

Enke N, Gemeinholzer B (2008) Babcock revisited: new insights into generic delimitation and character evolution in *Crepis* L. (Compositae: Cichorieae) from ITS and matK sequence data. Taxon 57:756–768

Euro + Med (2006–2018) Euro + Med PlantBase—the information resource for Euro-Mediterranean plant diversity. Available at: http://ww2.bgbm.org/EuroPlusMed/. Accessed Jan 2018

Fattorini S (2002) Biogeography of the tenebrionid beetles (Coleoptera, Tenebrionidae) on the Aegean Islands (Greece). J Biogeogr 29:49–67. https://doi.org/10.1046/j.1365-2699.2002.00656.x

Felsenstein J (1985) Confidence limits on phylogenies: an approach using the bootstrap. Evolution 39:783–791. https://doi.org/10.1111/j.1558-5646.1985.tb00420.x

Gould SJ (2002) The structure of evolutionary theory. The Belknap Press of Harvard University Press, Cambridge

Greuter W (1979) The origins and evolution of island floras as exemplified by the Aegean Archipelago. In: Bramwell D (ed) Plants and Islands. Academic Press, New York, pp 87–106

Heled J, Drummond AJ (2010) Bayesian inference of species tree from multilocus data. Molec Biol Evol 27:570–580. https://doi.org/10.1093/molbev/msp274

Kendall DG (1948) On the generalized "birth-and-death" process. Ann Math Stat 19:1–15

Kilian N, Gemeinholzer B, Lack HW (2009) Cichoriae. In: Funk VA, Susanna A, Stuessy TF, Bayer RJ (eds) Systematics, evolution and biogeography of the compositae. IAPT, Vienna, pp 343–383

Liveri L, Bareka P, Kamari G (2018) Taxonomic study on the Greek endemic genus *Hymenonema* (Asteraceae: Cichorieae), using morphological and karyological traits. Willdenowia 48:5–21. https://doi.org/10.3372/wi.48.48101

Meulenkamp JE, Sissingh W (2003) Tertiary palaeogeography and tectonostratigraphic evolution of the Northern and Southern Peri-Tethys platforms and the intermediate domains of the African-Eurasian convergent plate boundary zone. Palaeogeogr Palaeoclimatol Palaeoecol 196:209–228. https://doi.org/10.1016/S0031-0182(03)00319-5

Oberprieler C, Zimmer C, Bog M (2018) Are there morphological and life-history traits under climate-dependent differential selection in S Tunisian *Diplotaxis harra* (Brassicaceae) populations? Ecol Evol 8:1047–1062. https://doi.org/10.1002/ece3.3705

Petrova G, Moyankova D, Nishii K, Forrest L, Tsiripidis I, Drouzas AD, Djilianov D, Möller M (2015) The European paleoendmic *Haberlea rhodopensis* (Gesneriaceae) has an Oligocene origin and a Pleistocene diversification and occurs in a long-persisting refugial area in southeastern Europe. Int J Pl Sci 176:499–514. https://doi.org/10.1086/681990

Poulakakis N, Kapli P, Lymberakis P, Trichas A, Vardinoyiannis K, Sfenthourakis S, Mylonas M (2015) A review of phylogeographic analyses of animal taxa from the Aegean and surrounding regions. J Zool Syst Evol Res 53:18–32. https://doi.org/10.1111/jzs.12071

Rambaut A, Drummond AJ (2007) Tracer v1.4: MCMC trace analyses tool. Available at: http://beast.bio.ed.ac.uk/Tracer. Accessed 1 Oct 2018

Ree RH, Smith SA (2008) Maximum likelihood inference of geographic range evolution by dispersal, local extinction, and cladogenesis. Syst Biol 57:4–14. https://doi.org/10.1080/10635150701883881

Ronquist F, Huelsenbeck JP (2003) MrBayes 3: Bayesian phylogenetic inference under mixed models. Bioinformatics 19:1572–1574. https://doi.org/10.1093/bioinformatics/btg180

Ronquist F, Huelsenbeck J, Teslenko M (2011) Draft MrBayes version 3.2 manual: tutorials and model summaries. Available at: http://mrbayes.sourceforge.net/mb3.2_manual.pdf. Accessed 1 Oct 2018

Rydin C, Pedersen KR, Friis EM (2004) On the evolutionary history of *Ephedra*: Cretaceous fossils and extant molecules. Proc Natl Acad Sci USA 101:16571–16576. https://doi.org/10.1073/pnas.0407588101

Shaw J, Lickey EB, Schilling EE, Small RL (2007) Comparison of whole chloroplast genome sequences to choose noncoding regions for phylogenetic studies in angiosperms: the tortoise and the hare III. Amer J Bot 94:275–288. https://doi.org/10.3732/ajb.94.3.275

Simmons M, Ochoterena H (2000) Gaps as characters in sequence-based phylogenetic analyses. Syst Biol 49:369–381

Swofford DL (2002) PAUP*: phylogenetic analysis using parsimony (*and other methods). Version 4.0.b10. Sinauer Associates, Sunderland

Taberlet P, Gielly L, Pautou G, Bouvet J (1991) Universal primers for amplification of three non-coding regions of chloroplast DNA. Pl Molec Biol 17:1105–1109. https://doi.org/10.1007/BF00037152

Thompson JD (2005) Plant evolution in the mediterranean. Oxford University Press, Oxford

Thompson J, Higgins D, Gibson T (1994) CLUSTAL W: improving the sensitivity of progressive multiple sequence alignment through sequence weighting, positionspecific gap penalties and weight matrix choice. Nucl Acids Res 22:4673–4680

Tremetsberger K, Gemeinholzer B, Zetzsche H, Blackmore S, Kilian N, Talavera S (2013) Divergence time estimation in Cichorieae (Asteraceae) using a fossil-calibrated relaxed molecular clock. Organisms Diversity Evol 13:1–13. https://doi.org/10.1007/s13127-012-0094-2

Tremetsberger K, Ortiz MÁ, Terrab A, Balao F, Casimiro-Soriguer R, Talavera M, Talavera S (2016) Phylogeography above the species level for perennial species in a composite genus. AoB PLANTS 8:plv142. https://doi.org/10.1093/aobpla/plv142

White TJ, Bruns T, Lee S, Taylor J (1990) Amplification and direct sequencing of fungal ribosomal RNA genes for phylogenetics. In: Innis M, Gelfand D, Sninsky J, White T (eds) PCR protocols. A guide to methods and applications. Academic Press, San Diego, pp 315–322

Wright JJ, David SR, Near TJ (2012) Gene trees, species trees, and morphology converge on a similar phylogeny of living gars (Actinopertygii: Holostei: Lepidosteidae), an ancient clade of ray-finned fishes. Molec Phylogenet Evol 63:848–856. https://doi.org/10.1016/j.ympev.2012.02.033

Xie W, Lewis PO, Fan Y, Kuo L, Chen MH (2011) Improving marginal likelihood estimation for Bayesian phylogenetic model selection. Syst Biol 60:150–160. https://doi.org/10.1093/sysbio/syq085

Young ND, Healy J (2003) GapCoder automates the use of indel characters in phylogenetic analysis. BMC Bioinform 4:6. https://doi.org/10.1186/1471-2105-4-6

Yule GU (1924) A mathematical theory of evolution: based on the conclusions of Dr. J. C. Willis. Philos Trans Roy Soc London B Biol Sci 213:21–87. https://doi.org/10.1098/rstb.1925.0002